Two-stage dissipation in a superconducting microbridge: experiment and modeling

2010 Supercond. Sci. Technol. 23 085005

(http://iopscience.iop.org/0953-2048/23/8/085005)

Supercond. Sci. Technol. **23** (2010) 085005 (6pp) doi:10.1088/0953-2048/23/8/085005

Two-stage dissipation in a superconducting microbridge: experiment and modeling

L Del Río[1], E Altshuler[1], S Niratisairak[2], Ø Haugen[2], T H Johansen[2,3], B A Davidson[4], G Testa[5] and E Sarnelli[5]

[1] Superconductivity Laboratory, IMRE-Physics Faculty, University of Havana, 10400 Havana, Cuba
[2] Department of Physics, University of Oslo, 0316 Oslo, Norway
[3] Institute for Superconducting and Electronic Materials, University of Wollongong, Australia
[4] INFM-TASC Area Science Park, Basovizza, Italy
[5] Cybernetic Institute of the CNR, Via Campi Flegrei 34, 80078, Pozzuoli (NA), Italy

Received 13 April 2010, in final form 28 May 2010
Published 29 June 2010
Online at stacks.iop.org/SUST/23/085005

Abstract
Using fluorescent microthermal imaging we have investigated the origin of 'two-step' behavior in I–V curves for a current-carrying $YBa_2Cu_3O_x$ superconducting bridge. High resolution temperature maps reveal that as the applied current increases the first step in the voltage corresponds to local dissipation (hot spot), whereas the second step is associated with the onset of global dissipation throughout the entire bridge. A quantitative explanation of the experimental results is provided by a simple model for an inhomogeneous superconductor, assuming that the hot spot nucleates at a location with slightly depressed superconducting properties.

(Some figures in this article are in colour only in the electronic version)

1. Introduction

Jumps and other discontinuities in the current–voltage (I–V) characteristics of superconductors are commonly regarded as a fingerprint of failure. Their relevance for the behavior of superconducting magnets, storage coils and power transmission lines makes them a widely studied subject. While some kinds of discontinuities in I–V curves are claimed to be indications of self-organization in the dynamics of moving vortices in the presence of microscopic disorder [1–4], there is wide consensus that 'catastrophic' jumps are caused by resistive heating of macroscopic parts of the sample [5].

Local overheating can be associated with the appearance of finite regions of the superconductor becoming normal, coined 'hot spots' in a pioneering paper by Skocpol *et al* [6]. The authors proposed this idea as an explanation of the voltage-driven jumps observed in their experimental I–V curves measured on 'one-dimensional' bridges made from tin thin films. However, this is only one of many scenarios where hot spots can appear.

While the jumps in I–V curves associated with hot spots have an extraordinary importance for applications, a full understanding of the phenomenon demands the use of thermal visualization techniques. Low temperature scanning electron microscopy has been used to identify unstable hot spots generated by an electron beam in ultrathin NbN superconductors [7]. Hot spots in intrinsic stacks of Josephson junctions have been recently visualized in $Bi_2Sr_2CaCu_2O_8$ (BSCCO) superconductors by means of low temperature scanning laser microscopy [8]. Fluorescent thermal imaging (FTI) is a relatively simple technique that has been successfully used to visualize hot spots in $YBa_2Cu_3O_x$ (YBCO) microwave filters [9], YBCO thin film bridges [10] and BSCCO thin film bridges [11]. The available literature suggests that each type of material, working temperature, sample geometry and method of 'excitation' can generate hot spots with a variety of shapes and behaviors that are worth visualizing and modeling in each case.

In this work we make use of a serendipitous defect found in a thin film YBCO bridge to study and model a two-stage dissipation process. We report results from combined four-probe I–V measurements and visualization using FTI. Differently from previous studies, we are able to thermally visualize two distinct steps which are identified in the I–V curves. We also propose an ad hoc theoretical model for our specific experiment. For the two jumps found in the I–V

curve, we show that the first corresponds to the appearance of a localized hot spot in a defected region, and the second to the onset of an overall dissipation throughout the bridge. Besides reproducing our experimental observations with a minimum of free parameters, the model predicts hysteresis in the hot spot dynamics that may explain experimental measurements in previous reports [10–12].

2. Experimental results

The sample was a $d = 0.3$ μm thick c-axis oriented film of YBCO with a superconducting transition temperature of $T_c = 91$ K. The film was photo-lithographically patterned into a $w = 5$ μm wide and $l = 500$ μm long strip, which at both ends extends into large areas coated with gold for electrical connection. Space-resolved observation of the dissipation in the bridge was obtained using FTI, where a 1 μm thick film of poly(methyl-methacrylate) (PMMA) mixed with the fluorescent dye europium tris[3-(trifluoromethylhydroxymethylene)-(+)-camphorate] (EuTFC) deposited by spin coating on the sample, was used as sensor.

The FTI setup consists of a standard Leica DMR microscope and a Janis ST-500 continuous liquid helium flow cryostat, where the sample is mounted on the cold finger below an optical window (Suprasil) allowing incoming UV light to excite the fluorescent film, see figure 1. As UV-source we use a Hamamatsu LC6 with a 200 W mercury–xenon lamp equipped with an IR radiation filter and an optical light-guide. The dominant wavelength is at 365 nm providing a UV light intensity of 3 mW cm^{-2} on the sample area, which is found to give no measurable heating of the sample [12]. The light emitted from the sensor film has a strongly temperature-dependent intensity peak at 614 nm, and through a 10 nm bandpass filter in the microscope, an image recorded by a CCD camera allows a direct map of the temperature distribution to be created. The typical exposure time for the image recording is a few seconds.

The calibration of the system is performed by measuring the luminescence intensity over the range of interest by varying the cryostat temperature. With uniform conditions the temperature–intensity relation can be expressed as $\Delta T = \alpha_s \ln S$, where S is the ratio between the intensities measured at two temperatures differing by ΔT. The parameter α_s represents the sensitivity of the fluorescent film, and typically we find $\alpha_s \simeq 400$. The resolution is also determined by the bit depth of the CCD chip, and with our 12 bit camera it follows that the temperature sensitivity is 100 mK. Note that once the calibration is performed, the FTI-generated temperature maps will be based on image subtraction, i.e., intensity ratios pixel by pixel; $\Delta T(x_n, y_m) = \alpha \ln S(x_n, y_m)$, implying that the method largely compensates for local variations in the sensor film's thickness, the optical absorption etc. Further details about the FTI setup and the calibration procedure can be found in [12, 13]. The present experiments were carried out setting the cryostat temperature to $T_0 = 84$ K.

A stabilized dc-current source was used to apply the transport current in the bridge. The four-probe I–V measurements, and the recording of thermal images were performed simultaneously. Shown in figures 2(b) and (d), are thermal images of the sample carrying a current of 50 mA and 60 mA, respectively. Each thermal image is an average of 10 consecutive image recordings each taken with an exposure time of 1 s. Then the current was increased to a new plateau where a new average image again was obtained. For reference, figure 2(a) shows an optical image of the bridge. The unintentional defect in the film is easily seen in the image. Unfortunately, the sample was destroyed by an instance of over-dissipation before further characterization of the sample could be made.

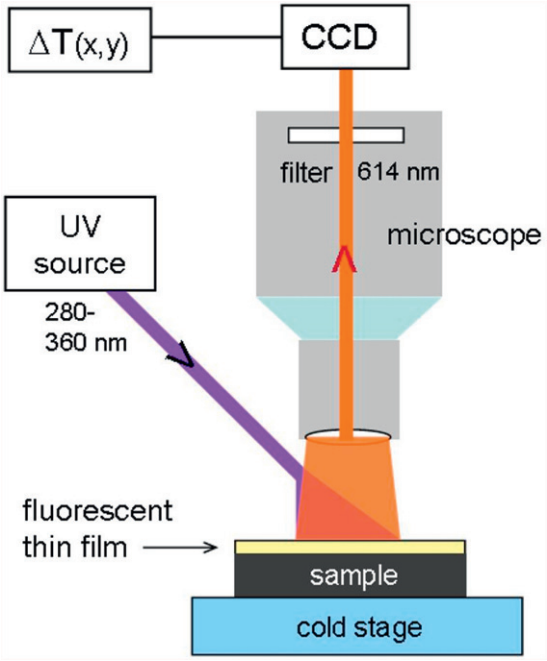

Figure 1. Experimental setup for microthermal imaging where a fluorescent polymer film serves as temperature sensor over the sample area.

The first evidence of heating was a hot spot appearing at $I = 50$ mA, as seen in the figure 2(b). The maximum temperature above the background was $\Delta T = 9$ K, which implies the temperature in the spot was just above T_c. Increasing the current produced a higher temperature at the hot spot, but did not cause any observable change in its size, in contrast to interpretations of other experiments [6]. We also found that the locally heated region was stable both in size and position, at least within the duration of each current plateau. Note in figure 2(b) that the faint 'shadow' along the bridge does not indicate a small temperature contrast, but drift in the positioning of the sample.

At $I = 60$ mA a second dramatic event took place. Now the entire bridge became normal, and with an average temperature elevation of $\Delta T = 80$ K. The center of the earlier hot spot continues to have the highest temperature, now with $\Delta T = 100$ K.

This two-stage process is also seen in the I–V curve shown in figure 3. A sudden increase in the voltage by $\Delta V_1 = 280$ mV at $I_{th1} = 45$ mA obviously corresponds to the formation of the hot spot seen in figure 2(b). The resistance

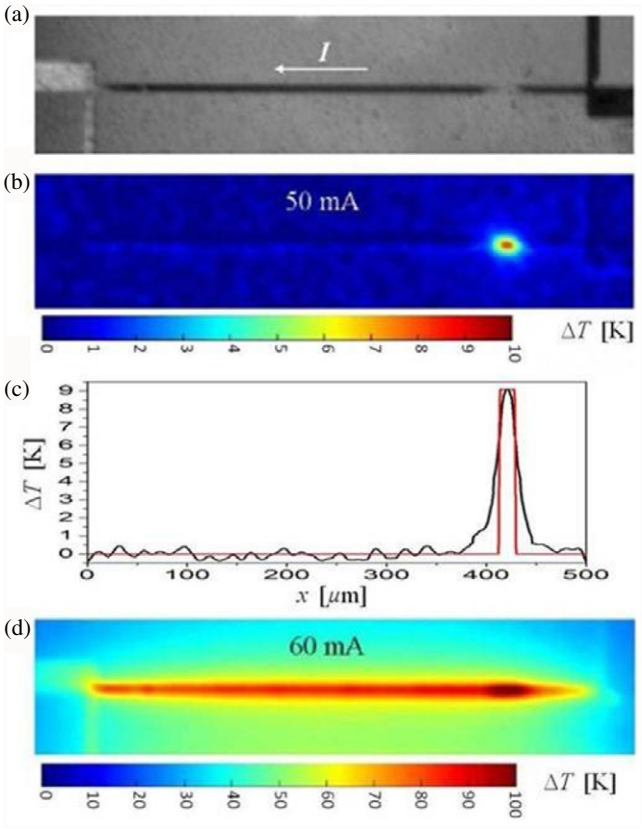

Figure 2. The bridge and its thermal evolution. (a) Optical image of the bridge, which is 0.5 mm long; (b) and (d) experimental thermal images for applied currents of 50 mA and 60 mA respectively (both of them have a color-coded scalebar where $\Delta T = 0$ corresponds to 84 K, the ambient temperature); (c) temperature profile along the center of the bridge (black and red lines correspond to experiment and theory, respectively).

of the hot spot is found to be $R_h = \Delta V_1/I_{th1} = 6.2\ \Omega$. The length of the hot spot is $\Delta x = 16\ \mu$m, determined as the width of the peak (distance between steepest flanks) in the line scan of the temperature distribution shown in figure 2(c).

As the current is increased further, the voltage grows linearly with a slope making the I–V curve extrapolate through origin. This constant resistance suggests a stable hot spot, as indeed was seen by the FTI, and a small variation of the resistivity within this range of current. Then at $I_{th2} = 57$ mA the voltage displays a second jump, which according to the thermal image at $I = 60$ mA, brings the whole bridge well into the normal state.

3. Modeling and discussion

Consider first the steady state behavior of the bridge at intermediate current values. Using the observation from our FTI microscopy that the size of the hot spot remains essentially constant, the I–V characteristics in the interval between the two threshold currents is expected to be described by

$$V = \frac{\rho_h \Delta x}{wd} I. \quad (1)$$

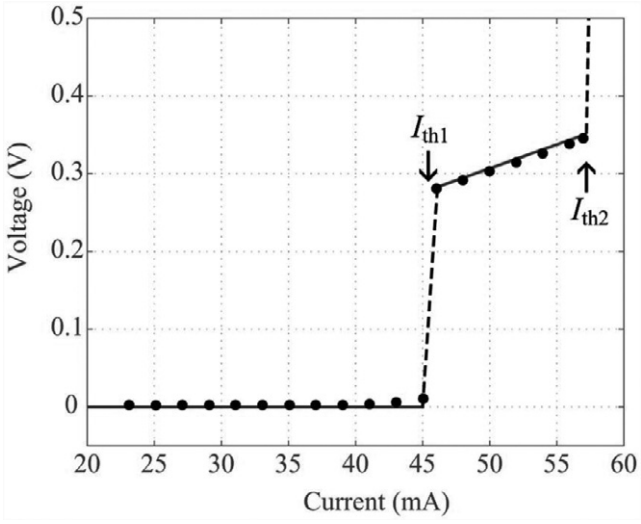

Figure 3. Current–voltage (I–V) characteristic of the bridge at 84 K showing voltage jumps at the threshold currents I_{th1} and I_{th2}. The voltage for $I = 60$ mA is higher than 20 V. The lines are fits based on equation (1).

The full line in figure 3 presents this linear relation, where the excellent fit is obtained using the observed Δx and a normal state resistivity of the hot spot region equal to $\rho_h = 6 \times 10^{-7}\ \Omega$ m.

To discuss the results in more detail a model was developed aiming to reproduce the full two-stage dissipation process, including the full spatial and temporal evolution. We consider the long thin superconducting strip as one-dimensional, along the x-axis. It is assumed that once a part of the strip becomes normal, that part will be a source of Joule heating. The heat then propagates in two different ways, (i) by thermal conduction along the strip, and (ii) by escaping into the environment according to the Newton law of cooling with an effective heat transfer coefficient, α. In the strip the temperature $T = T(x, t)$ then satisfies the following equation,

$$c\frac{\partial T}{\partial t} = k\frac{\partial^2 T}{\partial x^2} - \frac{\alpha}{d}(T - T_0) + \frac{I^2\rho(x)}{w^2 d^2}\Theta[T - T_c^*(x, I)], \quad (2)$$

with boundary conditions $T(0, t) = T(l, t) = T_0$. Here c is the specific heat per unit volume, k is the thermal conductivity and ρ is the normal state resistivity of the material. The unit step function, Θ, adds the Joule heating term only for x where T is above the local transition temperature T_c^*. Notice that T_c^* is not the thermodynamic critical temperature, but represents the line in the I–T plane separating states with pinned vortices from dissipative vortex states, i.e., the inverse of the temperature-dependent critical current $I_c(T)$. As suggests figure 7 in [14], we propose the following linear dependence of T_c^* on the applied current:

$$T_c^*(x, I) = T_c(x)(1 - I/I_0), \quad (3)$$

where I_0 is a fitting parameter. The samples' non-uniformity is modeled by using explicit coordinate dependencies of T_c and ρ, as shown in figure 4(a). This is motivated by comparing the direct image with the FTI images in figure 2, where

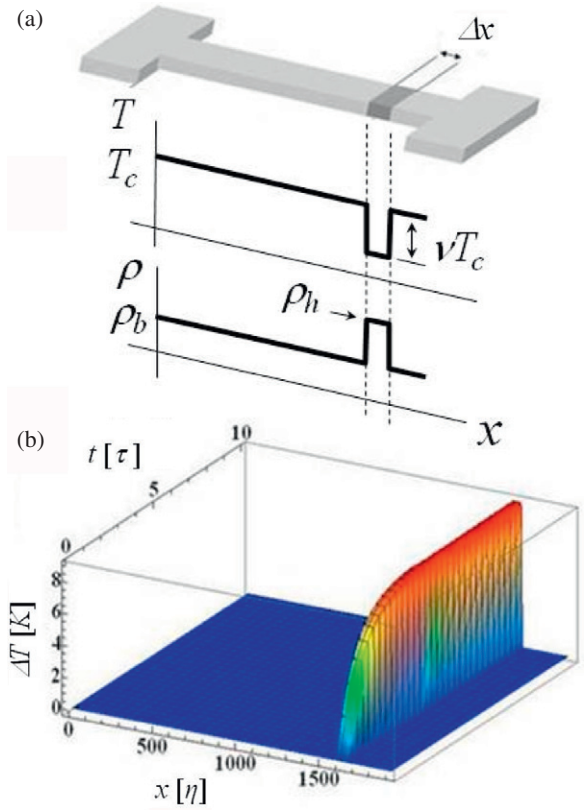

Figure 4. (a) Sketch of the superconducting bridge together with the profiles of critical temperature and resistivity. (b) Calculated temperature rise along the bridge after applying a current of $I = 50$ mA, causing formation of a hot spot (units on the axes are $\eta = \sqrt{kd/\alpha}$ and $\tau = cd/\alpha$, the characteristic length and time, respectively).

a correlation is evident between the hot spot position and the region of optical non-uniformity (of unknown origin, but clearly visible). Moreover, also a previous study [15] of a YBCO bridge where low temperature scanning electron microscopy was used to make a detailed T_c map, showed, when compared with magneto-optical images of the bridge while passing a supercritical current, that permanent damage is directly correlated with regions of depressed transition temperature.

The degree of non-uniformity is given by a suppression of T_c represented by the factor $\nu < 1$ and the excess resistivity $\Delta\rho = \rho_h - \rho_b$ in the defected zone, of size Δx. Here, and from now on, the index h stands for the weak zone and the index b for the rest of the bridge. The fact that the dimensions of the defect identified in figure 2 are close to the bridge width and much less than its length, justifies the present one-dimensional approximation.

As the applied current increases, dissipation will start in the region of depressed superconductivity at a threshold value, I_{th1}, determined by T_c^* of the defected region dropping to T_0. It follows from equation (3) that

$$I_{th1} = I_0[1 - T_0/(1-\nu)T_c]. \tag{4}$$

When the current is increased further, also T_c^* for the remaining part of the bridge eventually falls below T_0, and the whole strip starts to dissipate. This second threshold, I_{th2}, is given by

$$I_{th2} = I_0(1 - T_0/T_c). \tag{5}$$

From the experiment we observe that $I_{th1} = 45$ mA and $I_{th2} = 57$ mA, and we obtain $\nu = 0.017$ and $I_0 = 0.74$ A.

The form of equation (2) defines a characteristic length $\eta = \sqrt{kd/\alpha}$ and a transient time $\tau = cd/\alpha$ for spatial and temporal variations of the temperature profile. Provided that $\Delta x \gg \eta$ and the defected region is dissipating, the temperature is approximately uniform within each homogeneous part of the strip, as illustrated in figure 4(b), which represents the numerical solution of equation (2) for $I = 50$ mA. In particular, when passing an intermediate current $I_{th1} < I < I_{th2}$, it follows that the steady state temperature rise of the hot spot equals

$$\Delta T = \frac{I^2\rho_h}{w^2 d\alpha}. \tag{6}$$

With $\alpha = 2 \times 10^7$ W m^{-2} K^{-1}, a typical value reported in the literature for similar samples [16–18] we obtain an excess temperature $\Delta T = 9$ K at the hot spot, which agrees very well with the image in figures 2(b) and (c). Notice that, according to equation (6), for the range of current 45 mA $< I <$ 57 mA, corresponding to the existence of the hot spot, its temperature rise varies in the range 7.3 K $< \Delta T <$ 11.7 K, which translates into a small variation of 4.4 K around the mean value of 93.5 K of the absolute temperature of the hot spot. As we can see in [19], this consequently explains the small variation of the resistivity with temperature for this range of currents, in agreement with the comment made in the last paragraph of section 2.

As a check for consistency, note that with this value of α, and $k = 5$ W m^{-1} K^{-1} [20, 21], one finds $\eta = 0.26$ μm, which indeed satisfies $\eta \ll \Delta x$. With a specific heat of $c = 1.2 \times 10^6$ J m^{-3} K^{-1} [22], we find $\tau = 16$ ns, which is consistent with the fact that we do not observe any time evolution in the temperature distribution using the FTI method. It is worth noticing that, since our model assumes sharp parameter variations along the bridge, it cannot reproduce in detail the experimental temperature distribution shown in figure 2(c). However, it reproduces the overall features that allow one to explain the electrical behavior of the sample.

Our model also explains hysteresis in the I–V curves, which was found experimentally and reported elsewhere earlier [10, 11, 23]. Let us consider a process where the current is first increased to a maximum value above I_{th2}, and then decreased. To determine the thermal response of the system for a decreasing current, one has again to solve equation (2), but now with the initial condition given by the stationary solution at the maximum current corresponding to figure 2(d). The fact that $\Delta x \gg \eta$ implies the existence of two temperature levels along the bridge: one at the hot spot, and the other for the rest of the bridge. The temperature rises in the respective parts are

$$\Delta T_{b,h} = T_{b,h}(I/I_0)^2, \tag{7}$$

where $T_{b,h} = I_0^2\rho_{b,h}/w^2\,d\alpha$. We recall again that the index h is for the weak zone and the index b is for the rest of the bridge.

Since $\rho_h > \rho_b$, equation (7) indicates that the temperature increase in the damaged zone is bigger than in the rest of the bridge. Since the model assumes that $T_c^*(x, I)$ is larger outside the weak zone at any given current, a threshold I_{th3} exists for which the dissipation stops everywhere except in the weak section, which now becomes a localized hot spot. The threshold value is determined by the following equations, $T_c^* = T_c(1 - I_{th3}/I_0)$ and $\Delta T_b = T_c^* - T_0 = T_b(I_{th3}/I_0)^2$, leading to the result

$$I_{th3} = I_0 \frac{T_c}{2T_b}\left(\sqrt{1 + \frac{4T_b}{T_c}\frac{I_{th2}}{I_0}} - 1\right), \tag{8}$$

where I_{th2} is given by equation (5).

As we continue to decrease the current, one eventually reaches a threshold I_{th4} below which also the weak region becomes non-dissipative. I_{th4} is obtained similarly, with the result

$$I_{th4} = I_0 \frac{T_c'}{2T_h}\left(\sqrt{1 + \frac{4T_h}{T_c'}\frac{I_{th1}}{I_0}} - 1\right), \tag{9}$$

where I_{th1} is given by equation (4) and $T_c' = (1 - \nu)T_c$. From these equations it follows that $I_{th1} \geqslant I_{th4}$ and $I_{th2} \geqslant I_{th3}$ for any value of the parameters I_0, T_c, T_c', T_b and T_h. The equality only applies for the case of an ideal sample without thermal inertia where $\alpha \to \infty$.

Shown in figure 5 is the modeled I–V hysteresis loop for a quasi-static ramp of the current from zero to above I_{th2}, and then down to zero again. Every jump of voltage occurs at a threshold value I_{th_j} ($j = 1$–4) in the same sequence as the current is ramped. The voltage was calculated from

$$V(I) = \frac{I}{wd}\left[\rho_h \Delta x \Theta(I - I_{th1}) + \rho_b(l - \Delta x)\Theta(I - I_{th2})\right] \tag{10}$$

for the increasing current branch, and from

$$V(I) = \frac{I}{wd}\left[\rho_h \Delta x \Theta(I - I_{th4}) + \rho_b(l - \Delta x)\Theta(I - I_{th3})\right] \tag{11}$$

for the decreasing current branch.

We do not report any experimental I–V cycles for our specific sample, but we can compare qualitatively our theoretical results with previous experiments. Morgoon *et al* [23] obtained four-step hysteresis characteristics on YBCO twinned crystals (see curves 2 and 3 on figure 3 of [23]) which are qualitatively similar to the four-threshold loop predicted in our figure 5. This is not strange, considering that twinning defects constitute weak regions where hot spots can naturally occur. Haugen *et al* [10] obtained a simpler, two-step hysteresis curve (see figure 6 of [10]) for a YBCO thin film bridge. Thermal images of their sample do not show evidence of hot spots: the sample starts to dissipate more or less homogeneously along its length. The inset in our figure 5 suggests that two-threshold hysteresis, can also be associated with a hot spot, without necessarily reaching a 'full dissipation' state, provided the maximum applied current is smaller than I_{th2}. It then turns out that the observation of hysteresis in I–V curves without thermal imaging can easily lead to false conclusions on the dissipation mechanisms of a superconducting sample.

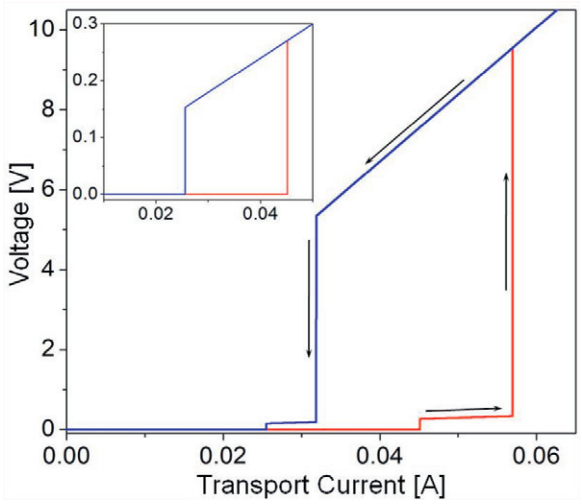

Figure 5. Calculated hysteresis loop for a slow variation of the current (the arrows indicate the ramping of the current). Every voltage jump takes place at a threshold value I_{th_j} ($j = 1$–4) in the same sequence as the current is ramped. In the inset is shown the hysteresis loop when the maximum applied current is smaller than $I_{th2} \approx 57$ mA.

4. Conclusions

We have reported *direct* observation of thermal maps suggesting that two-step I–V curves obtained when ramping up the current in non-homogeneous superconductors can be caused by the sudden appearance of a 'hot spot' in a region with depressed superconductivity, followed by a stage in which the whole bridge passes to the normal state. We have constructed a simple model of the sample consisting of a superconducting bridge with a finite region of depressed critical temperature and increased normal state resistivity. The model reproduces our increasing current, two-step experimental I–V curve, as well as the corresponding thermal maps. It also predicts four-step and two-step hysteresis in the I–V curves associated with hot spots, depending on the maximum applied current, which suggests that special care must be taken when driving conclusions about dissipation mechanisms solely based on transport experiments.

Acknowledgments

The authors acknowledge the financial support from the Norwegian Research Council, the Erasmus Mundus External Cooperation Window, the University of Havana's 'Alma Mater' research grants programme, and the Australian Research Council. Useful discussions with A J Batista-Leyva, O Sotolongo-Costa, R Jardim and S García are gratefully acknowledged. We thank C Pérez-Penichet for help in image processing. The Max Planck Institute for the History of Science and the International Center for Theoretical Physics (ICTP) provided access to relevant scientific journals, and M Arronte provided papers not available online.

References

[1] Olson C J, Reichhardt C and Nori F 1998 *Phys. Rev. Lett.* **80** 2197
[2] Bassler K E, Paczuski M and Altshuler E 2001 *Phys. Rev.* B **64** 224517
[3] Altshuler E and Johansen T H 2004 *Rev. Mod. Phys.* **76** 471
[4] Altshuler E, Johansen T H, Paltiel Y, Jin P, Bassler K E, Ramos O, Chen Q Y, Reinter G F, Zeldov E and Chu C W 2004 *Phys. Rev.* B **70** 140505
[5] Gurevich A Vl and Mints R G 1987 *Rev. Mod. Phys.* **59** 941
[6] Skocpol W J, Beasley M R and Tinkham M 1974 *J. Appl. Phys.* **45** 4054
[7] Doenitz D, Kleiner R, Koelle D, Scherer T and Shuster K F 2007 *Appl. Phys. Lett.* **90** 252512
[8] Wang H B, Guenon S, Yuan J, Iishi A, Arisawa S, Hatano T, Yamashita T, Koelle D and Kleiner R 2009 *Phys. Rev. Lett.* **102** 017006
[9] Hampel G, Kolodner P, Gammel P L, Polakos P A, de Obaldía E, Anderson A, Slattery R, Zhang D, Lian G C and Shih C F 1996 *Appl. Phys. Lett.* **69** 571
[10] Haugen Ø, Johansen T H, Chen H, Yurchenko V, Vase P, Winkler D, Davidson B A, Testa G, Sarnelli E and Altshuler E 2007 *IEEE Trans. Appl. Supercond.* **17** 3215
[11] Niratisairak S, Haugen Ø, Johansen T H and Ishibahi T 2008 *Physica* C **468** 442
[12] Haugen Ø 2008 High-resolution fluorescence thermal imaging at cryogenic temperatures *PhD Thesis* The University of Oslo, p 52
[13] Haugen Ø and Johansen T H 2008 *J. Lumin.* **128** 1479
[14] Dale S J, Wolf S M and Schneider T R (ed) 1990 *Energy Applications of High-Temperature Superconductivity, Detailed Assesment* vol 2 (Palo Alto, CA: Electric Power Research Institute) pp 1–19
[15] Gaevski M E, Johansen T H, Bratsberg H, Galperin Y M, Bobyl A V, Shantsev D V and Karmanenko S F 1997 *Appl. Phys. Lett.* **71** 3147
[16] Nahum M, Verghese S, Richards P L and Char K 1991 *Appl. Phys. Lett.* **59** 2034
[17] Xiao Z L, Andrei E Y and Ziemann P 1998 *Phys. Rev.* B **58** 11185
[18] Zeuner S, Lengfellner H and Prettl W 1995 *Phys. Rev.* B **51** 11903
[19] Abdelhadi M M and Jung J A 2003 *Phys. Rev.* B **68** 184515
[20] Marshall C D, Fishman I M and Fayer M D 1991 *Phys. Rev.* B **43** 2696
[21] Hagen S J, Wang Z Z and Ong N P 1989 *Phys. Rev.* B **40** 9389
[22] Heatinger C, Abrego Castillo I, Kunzler J V, Ghivelder L, Pureur P and Reich S 1996 *Supercond. Sci. Technol.* **9** 639
[23] Morgoon V N, Jardim R F, Bindilatti V, Becerra C C, Rodrigues D Jr, Bondarenko A V and Sivakov A V 1996 *J. Supercond.* **9** 129